Inorganic Chemistry

ARTICLE

pubs.acs.org/IC

Designed Iron Carbonyls as Carbon Monoxide (CO) Releasing Molecules: Rapid CO Release and Delivery to Myoglobin in Aqueous Buffer, and Vasorelaxation of Mouse Aorta

Margarita A. Gonzalez,[†] Nicole L. Fry,[†] Richard Burt,[‡] Riddhi Davda,[‡] Adrian Hobbs,*[,‡] and Pradip K. Mascharak*[,†]

[†]Department of Chemistry and Biochemistry, University of California, Santa Cruz, California 95064, United States

[‡]Department of Pharmacology, University College, London WC1E 6BT, U.K.

Supporting Information

ABSTRACT: The physiological roles of CO in neurotransmission, vasorelaxation, and cytoprotective activities have raised interest in the design and syntheses of CO-releasing materials (CORMs) that could be employed to modulate such biological pathways. Three iron-based CORMs, namely, $[(PaPy_3)Fe(CO)](ClO_4)$ (**1**), $[(SBPy_3)Fe(CO)](BF_4)_2$ (**2**), and $[(Tpmen)Fe(CO)](ClO_4)_2$ (**3**), derived from designed polypyridyl ligands have been synthesized and characterized by spectroscopy and X-ray crystallography. In these three Fe(II) carbonyls, the CO is trans to a carboxamido-N (in **1**), an imine-N (in **2**), and a tertiary amine-N (in **3**), respectively. This structural feature has been correlated to the strength of the Fe-CO bond. The CO-releasing properties of all three carbonyls have been studied in various solvents under different experimental conditions. Rapid release of CO is observed with **2** and **3** upon dissolution in both aqueous and nonaqueous media in the presence and absence of dioxygen. With **1**, CO release is observed only under aerobic conditions, and the final product is an oxo-bridged diiron species while with **2** and **3**, the solvent bound $[(L)Fe(CO)]^{2+}$ (where L = $SBPy_3$ or Tpmen) results upon loss of CO under both aerobic and anaerobic conditions. The apparent rates of CO loss by these CORMs are comparable to other CORMs such as $[Ru(glycine)(CO)_3Cl]$ reported recently. Facile delivery of CO to reduced myoglobin has been observed with both **2** and **3**. In tissue bath experiments, **2** and **3** exhibit rapid vasorelaxation of mouse aorta muscle rings. Although the relaxation effect is not inhibited by the soluble guanylate cyclase inhibitor ODQ, significant inhibition is observed with the BK_{Ca} channel blocker iberiotoxin.

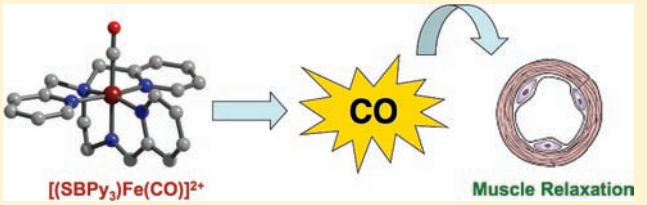

INTRODUCTION

During the past three decades, three small "toxic" molecules namely nitric oxide (NO), carbon monoxide (CO), and hydrogen sulfide (H_2S) have drawn much attention because of their surprising and unexpected roles in numerous physiological processes.[1] The surge of interest in these "biologically relevant gases" all began with NO. What once was viewed as an environmental pollutant, NO, has now been shown to participate in a myriad of physiological and pathological processes including vasodilation,[2] neurotransmission,[3] immune response,[4] and cellular apoptosis.[5] More recently, CO and H_2S have also been identified as important signaling molecules.[1,6,7] While the role of NO in several biological pathways has been established firmly, research on the mechanistic role of H_2S is in its infancy. Among this series of gasotransmitters, NO and CO possess the greatest number of similarities—both known to interact with metalloproteins, particularly those bearing heme moieties.[8] Consequently, the biological relevance of CO, an endogenously produced gaseous molecule, has been emerging at a faster rate during the past few years.[9,10] The bulk of CO in tissues and cells is generated from the catabolism of heme by heme oxygenase (HO)[11] while minor amounts are derived from iron-catalyzed lipid peroxidation. CO, like NO, has been implicated in regulatory functions including neurotransmission, vasorelaxation, and cytoprotective activity. For instance, while NO is known to have a greater binding affinity for soluble guanylyl cyclase (sGC),[12] it has been determined that sGC is able to bind CO thus supporting the notion of CO-mediated vasorelaxation through cGMP attenuation.[9,12] Other pathways for CO-mediated signaling include a cytochrome p450-based monooxygenase system,[13] and modulation of K^+-channels.[14] Perhaps the most interesting feature of CO is its ability to exert cytoprotective action. CO has been found to protect against hyperoxic lung injury,[15] organ transplant rejection,[16] and to promote mitochondrial biogenesis.[17]

To effectively induce the desirable biological effects of CO at a targeted site, controlled site-specific delivery of CO to tissues is

Received: January 13, 2011
Published: March 08, 2011

required and the product after CO-release must remain benign. CO is a ubiquitous ligand in organometallic chemistry. Not surprisingly, the early CORMs were mostly homo and heteroleptic transition metal carbonyls (CO complexes) such as $[Fe(CO)_5]$, $[Mn_2(CO)_{10}]$, and $[\{Ru(CO)_3Cl_2\}]_2$.[18] The kinetics (and trends) of CO release from metal carbonyls (M = Cr, Mo, W) upon solvation has been studied by Lynam and coworkers.[19] These prototypical carbonyls manifested CO delivery to substrates, with the limitation of only being soluble in aprotic solvents, particularly dimethylsulfoxide (DMSO). $[Ru(glycine)(CO)_3Cl]$, developed by Motterlini and co-workers (and often referred to as CORM-3), was one of the first compounds to be found soluble in aqueous media.[20] This CORM effectively mimics the vasorelaxing and cardioprotective properties associated with CO produced endogenously.[20−22] Further efforts in preparing metal carbonyls as therapeutics focused on the incorporation of a biocompatible ligand to facilitate CO delivery. As nontoxic leaving groups, amino acids and amino esters have been utilized as ligands in the preparation of group 6-based CORMs.[23] The involvement of 2-pyrone functionalities in metabolic pathways has also led to the syntheses of Fe and Mo-based CORMs bearing a pyrone moiety.[24] As with all of the previously reported CORMs, these carbonyls release CO rapidly upon dissolution. In a recent account, Schatzschneider and coworkers have reported a tricarbonyl complex $[Mn(CO)_3(tmp)](PF_6)$ [tmp = tris(pyrazolylmethane)] that releases CO upon irradiation with UV light.[25,26] The limited applicability of the reported metal carbonyls in CO delivery to biological targets has, however, kept the search for new water-soluble CORMs with predictable CO-releasing properties ongoing.

Previously, we have reported several designed metal nitrosyls (NO complexes of metals such as Fe, Mn, and Ru) that rapidly deliver NO upon exposure to lights of a wide range of wavelengths (400−1000 nm).[27−32] Such NO donors have been employed to inhibit enzymes,[33] trigger apoptosis in human breast cancer cells,[34] and eradicate pathogenic bacteria[35] under the control of light. To explore whether the design principles could be utilized in synthesizing CORMs, we have now investigated the CO-releasing behavior of three iron carbonyls derived from three pentadentate polypyridine ligands shown in Figure 1. These ligands are expected to stabilize Fe(II) centers and allow CO binding. Although the synthesis and structure of the Fe(II) carbonyl derived from *N,N′*-bis(2-pyridyl-methyl)amine-*N*-ethyl-2-pyridine-2-carboxamide ($PaPy_3H$), namely, $[(PaPy_3)Fe(CO)](ClO_4)$ (**1**), were reported by us in a previous account,[36] the CO-releasing property was not studied. In the present work, we have synthesized and characterized two more Fe(II) carbonyls derived from related ligands, namely, *N,N′*-bis(2-pyridylmethyl)amine-N-ethyl-2-pyridine-2-aldimine ($SBPy_3$) and *N*-methyl-*N,N′,N′*-tris(2-pyridylmethyl)ethane-1,2-diamine (Tpmen). In the structurally related series $[(PaPy_3)Fe(CO)](ClO_4)$ (**1**), $[(SBPy_3)Fe(CO)](BF_4)_2$ (**2**), and $[(Tpmen)Fe(CO)](ClO_4)_2$ (**3**), the design allowed us to place CO trans to a carboxamido-N (strong σ-donor), an imine-N (moderately π-accepting) and a tertiary amine-N (weak σ-donor) center, respectively. The structures of **2** and **3** and their spectroscopic properties are reported in this paper. All three carbonyls are soluble in aqueous buffers and rapidly release CO in such solutions. The CO-releasing parameters of **1**−**3** have been carefully evaluated both in acetonitrile (in presence and absence of dioxygen) and in aerated aqueous phosphate buffer. The extent of CO release from **2** and **3** has been assessed using myoglobin assay under physiological conditions. Finally, the utility of these new CORMs has been demonstrated in relaxation of mouse aortic smooth muscle tissue in vitro, and the possible pathways of CO-mediated relaxation are discussed.

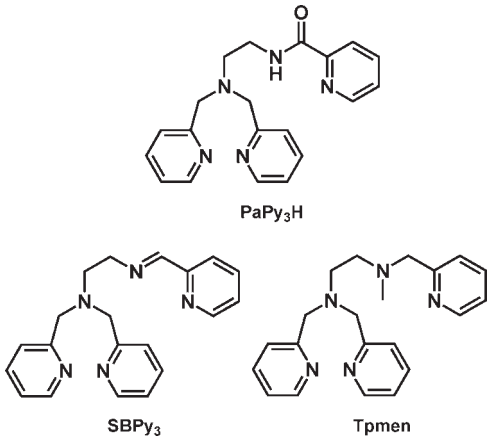

Figure 1. Structures of the designed ligands used in this study.

EXPERIMENTAL SECTION

Materials. Iron(II) tetrafluoroborate hexahydrate and Iron(II) perchlorate hydrate were purchased from Aldrich Chemical Co. and used without further purification. CO was procured from Praxair. Horse heart myoglobin (Mb) was purchased from Aldrich and used as received. All solvents were dried by standard techniques and distilled prior to use. The ligands $SBPy_3$ and Tpmen were synthesized according to the literature procedures.[37,38] The Fe(II) starting salt $[Fe(MeCN)_4](ClO_4)_2$, was also synthesized by following the published procedure.[39]

. ***Caution!*** *Complexes of transition metal perchlorates with organic ligands are hazardous and may explode upon heating. Only small quantities must be handled with the proper protection.*

Syntheses of Compounds. *$[(SBPy_3)Fe(CO)](BF_4)_2$ (**2**).* Under dinitrogen, a solution of 0.415 g (0.99 mmol) of $[Fe(MeCN)_4](ClO_4)_2$ in 10 mL of MeOH was slowly added to a solution of 0.332 g (0.98 mmol) of $SBPy_3$ ligand in 20 mL of MeOH, and the deep purple solution was stirred for the next 1 h. Next, CO was bubbled through the solution when complex **2** separated out as a red solid within 3−5 min. The red solid thus obtained was filtered, washed with Et_2O, and dried in vacuo (0.592 g, 60% yield). Crystals of $[(SBPy_3)Fe(CO)](BF_4)_2$, suitable for X-ray diffraction, were grown by redissolving **2** in MeOH and storing under CO atmosphere at −20 °C for 24 h. Anal. Calcd for $C_{21}H_{21}N_5OB_2F_8Fe$: C, 42.83; H, 3.59; N, 11.89. Found: C, 42.80; H 3.48; N, 11.94. Selected IR frequencies (cm^{-1}, KBr disk): 2010 (vs ν_{CO}), 1471 (w), 1053 (vs), 771 (s).

*$[(Tpmen)Fe(CO)](ClO_4)_2$ (**3**).* A solution of 0.121 g (0.35 mmol) of Tpmen ligand in 30 mL of MeOH was degassed by freeze−pump−thaw cycles. To the frozen solution of the ligand, a batch of 0.144 g (0.35 mmol) of $[Fe(MeCN)_4](ClO_4)_2$ was added as a solid. The frozen solution was warmed to room temperature in a warm water bath, and the clear yellow solution was stirred under dinitrogen at room temperature for 1 h. Next, CO was bubbled through the solution when complex **3** separated as a beige solid within 5−10 min. The solid was filtered, washed with Et_2O, and dried under vacuo (0.083 g, 38% yield). X-ray quality crystals of $[(Tpmen)Fe(CO)](ClO_4)_2$ were grown by redissolving **3** in MeOH and storing under CO at −20 °C for 24 h. Anal. Calcd for $C_{22}H_{25}N_5O_9Cl_2Fe$: C, 41.93; H, 4.00; N, 11.12. Found: C, 41.88; H

dx.doi.org/10.1021/ic2000848 |*Inorg. Chem.* 2011, 50, 3127–3134

Table 1. Summary of Crystal Data, Intensity Collection, and Refinement Parameters for $[(SBPy_3)Fe(CO)](BF_4)_2$ (2)

empirical formula	$C_{21}H_{21}N_5OB_2F_8Fe$
formula weight	588.90
crystal color	red blocks
crystal size (mm^3)	0.04 × 0.03 × 0.03
temperature (K)	150(2)
wavelength (Å)	0.77490
crystal system	orthorhombic
space group	$Pca2_1$
a (Å)	12.9790(5)
b (Å)	12.2232(5)
c (Å)	15.0473(5)
α (deg)	90.00
β (deg)	90.00
γ (deg)	90.00
V ($Å^3$)	2387.18(16)
Z	4
d_{cal} (g/cm^3)	1.639
μ (mm^{-1})	0.852
GOF[a] on F^2	1.036
final R indices	R_1 = 0.0648
$[I > 2\sigma(I)]$	wR_2 = 0.1766
R indices[b]	R_1 = 0.0833
all data[c]	wR_2 = 0.1952

[a] GOF = $[\Sigma[w(F_o^2 - F_c^2)^2]/(N_o - N_v)]^{1/2}$ (N_o = number of observations, N_v = number of variables). [b] $R_1 = \Sigma||F_o| - |F_c||/\Sigma|F_o|$. [c] $wR_2 = [\Sigma w(F_o^2 - F_c^2)^2/\Sigma w(F_o^2)]^{1/2}$.

Table 2. Selected Bond Distances (Å) and Angles (deg) for $[(SBPy_3)Fe(CO)](BF_4)_2$ (2)

Fe−C21	1.805(7)
C21−O1	1.122(8)
Fe−N1	1.968(5)
Fe−N2	1.968(5)
Fe−N3	2.003(5)
Fe−N4	1.926(5)
Fe−N5	1.998(5)
Fe−C21−O1	177.9(6)
C21−Fe−N4	176.5(3)

4.02; N, 10.77. Selected IR frequencies (cm^{-1}, KBr disk): 2012 (vs ν_{CO}), 1472 (w), 1093 (vs), 771 (s), 624 (s).

Physical Measurements. Electronic absorption spectra were recorded on a Varian Cary 50 Spectrophotometer. Infrared Spectra were obtained by using a Perkin-Elmer 1600 FTIR Spectrophotometer. Room temperature magnetic susceptibility values were measured by using a Johnson Matthey magnetic susceptibility balance. Diffraction data for **2** was collected at 150 K on a D3 goniostat equipped with a Bruker APEXII CC detector at Beamline 11.3.1 at the Advanced Light Source (Lawrence Berkeley National Laboratory) using synchrotron radiation tuned to λ = 0.7749 Å. The data frames were collected using the program APEX2 v2010.3.0 and processed using the program SAINT v7.60A within APEX2. The data were corrected for absorption and beam corrections based on the multiscan technique as implemented in SADABS. Diffraction data for **3** was collected at 150 K on a Bruker APEX-II instrument using monochromated Mo−Kα radiation (λ = 0.71073 Å) and corrected for absorption. The structure was solved using direct methods (standard SHELXL-97 package). Machine parameters, crystal data, and data collection parameters for **2** are summarized in Table 1 while selected bond distances and angles are listed in Table 2. Complete crystallographic data for **2** have been submitted as Supporting Information. Because of extensive disorder of the perchlorate counterions and one enantiomer of complex **3** in the lattice, the final refinement of the structure of **3** presented problems. At this time, we have the preliminary structure that clearly depicts the overall connectivity of the atoms (see Supporting Information, Figure S1). The final structure will be reported in due time.

Measurements on the Apparent CO-Release Rate in Solution. About 0.5−1 mg of **2** or **3** was placed in a quartz cuvette, and 1 mL of solvent was added. The mixture was shaken to ensure complete dissolution, and absorbance was recorded immediately. The rates of CO release of **2** and **3** were determined by monitoring the decrease in absorption at the λ_{max} of each compound in either MeCN or PBS (100 mM, pH 7.4). The plots were fitted to the three parameter exponential equation $A(t) = A_\infty + (A_o - A_\infty)\exp\{-k_{CO}t\}$, where A_o and A_∞ are the initial and final absorbance values, respectively. The apparent rate of CO loss (k_{CO}) was calculated from the $\ln(C)$ versus time plot for each CORM.

Delivery of CO to Myoglobin. Horse heart myoglobin was dissolved in phosphate buffered saline (PBS, 100 mM, pH 7.4) and reduced by adding sodium dithionite. The concentration of the deoxymyoglobin (Mb) generated was calculated from the absorbance of the Soret band at 435 nm (extinction coefficient = 121 mM^{-1} cm^{-1}). On the basis of the Mb concentration, we added a PBS solution of either **2** or **3** to the Mb solution, and the initial absorbance was taken within 1 min. Carbonyl myoglobin (Mb-CO) production was monitored over time. A shift in λ_{max} from 435 to 424 nm was observed in each case because of formation of the Mb-CO. Final concentrations of Mb-CO were assessed at 424 nm (extinction coefficient =207 mM^{-1} cm^{-1}) and compared to the initial Mb present in solution to quantify CO release by each compound.

CO Delivery to Mouse Aorta. Male C57BLK6 mice (25−35 g) were stunned and killed by cervical dislocation. The thoracic aorta was carefully removed, cleaned of connective tissue, and cut into three to four ring segments of approximately 4 mm in length. Aortic rings were mounted in 10 mL organ baths containing Krebs-bicarbonate buffer (composition (mM): Na^+ 143; K^+ 5.9; Ca^{2+} 2.5; Mg^{2+} 1.2; Cl^- 128; HCO_3^- 25; HPO_4^{2-} 1.2; SO_4^{2-} 1.2; D-glucose 11) maintained at 37 °C and gassed with 95% O_2/5% CO_2. Tension was initially set at 0.3 g and reset at intervals following an equilibration period of 1 h during which time fresh Krebs-bicarbonate buffer was replaced every 15−20 min. After equilibration, the rings were primed with KCl (48 mM), washed, and precontracted phenylephrine (PE, 1 μM) was added. Once this response had stabilized, acetylcholine (ACh, 1 μM) was added to the bath to assess the integrity of the endothelium. If the contractions to PE were not maintained, or relaxations greater than 50% of the PE-induced tone to ACh were not observed, the tissues were discarded.

Tissues were then washed for 30 min (by addition of fresh Krebs-bicarbonate buffer at 15 min intervals) after which cumulative concentrations of PE (1 nM−1 μM) were added to the organ bath. The tissues were then washed over 60 min to restore basal tone before contracting to approximately 80% of the maximum PE-induced response. Once a stable response to PE was achieved, cumulative concentration−response curves to **2** (30 nM−100 μM) and **3** (30 nM−300 μM) were constructed.

To determine the role of soluble guanylate cyclase (sGC) in the vasorelaxant response to the CO-donors, concentration−response curves to both **2** and **3** were constructed in tissues in the absence or presence of the sGC inhibitor ODQ (1H-[1,2,4]oxadiazolo[4,3-a]quinoxalin-1-one, 5 μM). To investigate the effect of K^+-channel activation in the vasorelaxant response to the CO-donors, concentration−response curves to **3** were constructed in tissues in the absence or presence of the large-conductance calcium-activation K^+-channel

dx.doi.org/10.1021/ic2000848 |*Inorg. Chem.* 2011, 50, 3127–3134

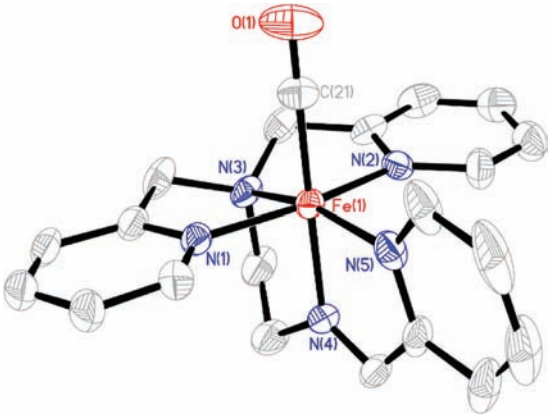

Figure 2. Thermal ellipsoid (probability level 30%) plot of $[(SBPy_3)Fe(CO)]^{2+}$ (cation of **2**) with the atom labeling scheme. H atoms have been omitted for the sake of clarity.

(BK_{Ca}) blocker iberiotoxin (100 nM), the K_{ATP} channel blocker glibenclamide (10 μM), and the nonselective K^+-channel blocker tetraethylammonium (TEA; 3 mM) ion.

RESULTS AND DISCUSSION

Reactions of the pentadentate ligands of Figure 1 with $[Fe(MeCN)_4](ClO_4)_2$ in MeOH results in formation of the solvent-bound species $[(L)Fe(MeOH)]^{n+}$ which upon exposure to CO affords the desired Fe(II) carbonyls **1**−**3**. In case of $PaPy_3H$, the presence of a base (Et_3N) is required for deprotonation of the carboxamide group.[36] The presence of the solvent-bound species in these reactions has been confirmed by the isolation and structural characterization of $[(SBPy_3)Fe(MeCN)](BF_4)_2$ when $SBPy_3$ is allowed to react with $[Fe(MeCN)_4](ClO_4)_2$ in MeCN.[37] Replacement of the bound solvent molecule with CO is quite rapid, and the carbonyls crystallize out of the MeOH solutions when kept under CO atmosphere at low temperature. In solid state, all three carbonyls are indefinitely stable at room temperature.

A strong CO stretch (ν_{CO}) at 1972 (for **1**), 2010 (for **2**), and 2012 (for **3**) cm^{-1} confirms the presence of bound CO ligand in the three carbonyls. These ν_{CO} values are within the range noted for other Fe(II) complexes with Fe(II)-CO bonds. For example, *trans*-[(TPP)Fe(1-MeIm)(CO)] (where TPP = 5,10,15,20-tetraphenylporphinate ligand, 1-MeIm = I-methylimidazole)[40] exhibits its ν_{CO} at 1969 cm^{-1} while *trans*-$[(DPGH)_2Fe(py)(CO)]$ (where DPGH = bidentate diphenylglyoximato univalent anion)[41] displays its ν_{CO} at 1996 cm^{-1}. Comparison of the ν_{CO} values of structurally similar carbonyls **1**−**3** reveals an interesting trend. The change from a strong σ-donating and negatively charged carboxamido-N donor in **1** to a neutral (and moderately π-accepting) imine-N or weak tertiary-N donor (in **2** and **3** respectively), increases the ν_{CO} value from 1972 to 2010−2012 cm^{-1}. This increase in ν_{CO} value clearly demonstrates that as more electron density is pushed toward the Fe(II) center, it transfers part of the electron density to the antibonding orbital of the bound CO ligand trans to it (as is the case in **1**). Such transfer strengthens the Fe−C(O) bond in **1** more than the other two carbonyls and makes it a slow CO-releasing molecule (vide infra).

The low-spin configuration of the Fe(II) center in **1**−**3** has been confirmed by their diamagnetism in solid state. The

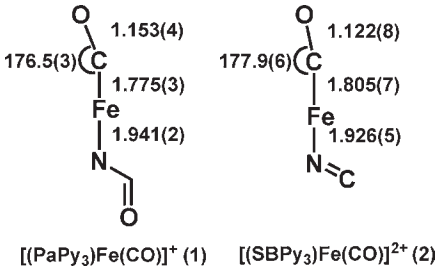

Figure 3. Comparison of the metric parameters and axial coordination of **1** and **2**.

Mössbauer parameters (δ = 0.15 mm s^{-1}, $|\Delta E_Q|$ = 0.74 mm s^{-1}) of **1** also corroborate this assignment.[36] Out of the three carbonyls, only **1** does not lose CO in degassed aprotic solvents like MeCN. This fact allowed us to acquire a clean ^1H NMR spectrum in CD_3CN in our previous study.[36]

Structures of the Complexes. $[(SBPy_3)Fe(CO)](BF_4)_2$ (2). The structure of $[(SBPy_3)Fe(CO)]^{2+}$, cation of **2**, is shown in Figure 2, and selected metric parameters are listed in Table 2. The Fe(II) center is situated in an octahedral environment with the imine N trans to CO, while the remaining N donors (three pyridine-N and one tertiary amine-N) are in the equatorial plane. Much like **1**, the Fe−C(O) bond angle is almost linear (176.5(3)°). Similar Fe−C(O) bond angles have been noted with other low-spin Fe(II) carbonyl complexes such as *trans*-[-$(DPGH)_2Fe(py)(CO)]$ (178°).[41]

Comparison of the structural parameters of **2** with that of **1** reveals interesting similarities and differences (Figure 3). The Fe−C(O) bond distance observed for **2** (1.805(7) Å) is noticeably longer than that observed in **1** (1.775(3) Å). The C−O bond length in **2** (1.122(8) Å) is, however, shorter than that in **1** (1.153(4) Å). The elongated Fe−C(O) and shorter C−O bond distances observed in **2** suggest a reduced degree of π-back-bonding in this complex compared to **1**. The $Fe-N_{imine}$ bond length of 1.926(5) Å further supports reduced backbonding character in **2**, as the imine group is able to accept electron density from the metal center. These structural parameters are consistent with the facile CO release observed with **2** (vide infra).

$[(Tpmen)Fe(CO)](ClO_4)_2$ (3). As mentioned above, the structure of **3** has not been fully characterized because of disorder problems in the crystal lattice. Exchange of counterions did not provide any respite. In the *preliminary structure* of the perchlorate salt, the connectivity of atoms, however, is quite clear (Supporting Information, Figure S1). The CO is trans to the tertiary amine-N while three pyridyl-Ns and the second tertiary N (with CH_3 group attached to it) are coordinated to the iron center in the equatorial plane.

Electronic Absorption Spectra and CO-Release in Solution. In the present study, the behavior of **1**−**3** in solution has been studied in detail to evaluate their capacity as CORMs. The electronic absorption spectra of **1**−**3** have been acquired in MeCN and phosphate buffer (PBS, pH = 7.4) via rapid dissolution and quick data collection. The color of the solutions of all the carbonyls intensifies upon loss of CO and significant changes with distinct isosbestic points are noted in their electronic absorption spectra. For example, **2** exhibits a strong metal-to-ligand charge transfer (MLCT) band with λ_{max} at 455 nm in MeCN which shifts to 555 nm upon CO release and the color changes from red to deep magenta. Clean isosbestic points are noted at 485, 415, and 340 nm (Supporting Information, Figure S2). The final spectrum (obtained

dx.doi.org/10.1021/ic2000848 |*Inorg. Chem.* 2011, 50, 3127–3134

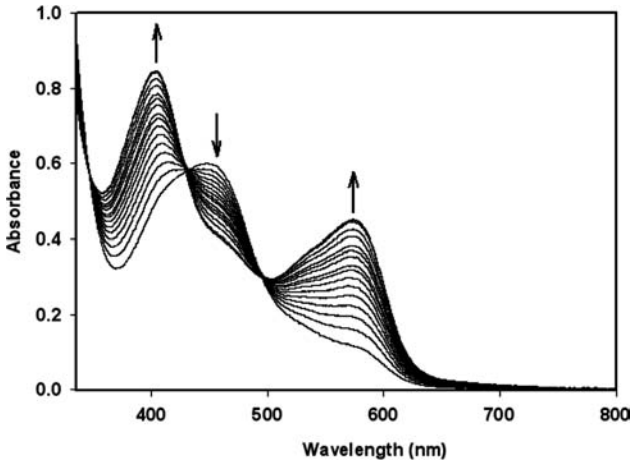

Figure 4. Electronic absorption spectrum of $[(SBPy_3)Fe(CO)](BF_4)_2$ (**2**) in 0.1 M PBS, pH 7.4 (concentration of **2** = 3.5 mM).

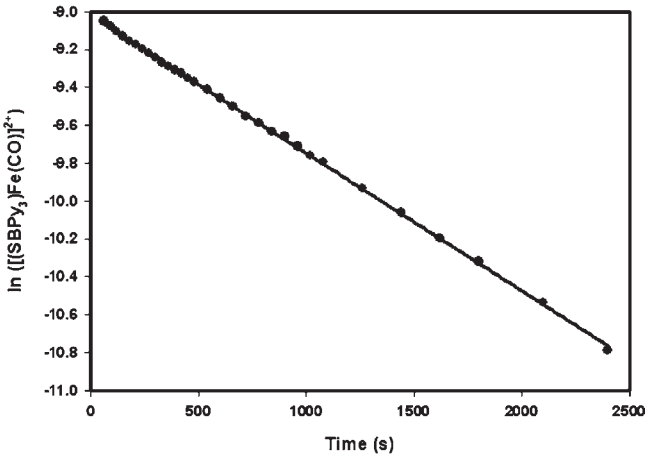

Figure 5. Plot of changes in ln[**2**] versus time(s) in 0.1 M PBS, pH 7.4 as monitored by noting the absorbance values at 450 nm.

within 15 min) is identical to that of $[(SBPy_3)Fe(MeCN)](BF_4)_2$, a structurally characterized species reported by us previously.[37] The red shift of the MLCT band upon loss of CO clearly indicates that the electron density from the antibonding π^* orbital of bound CO ligand returns back to the Fe(II) center in $[(SBPy_3)Fe(MeCN)]^{2+}$. With **3**, the initial yellow color deepens because of similar red shift of the MLCT band from 330 to 390 nm (isosbestic points at 352 and 242 nm) and the final spectrum of $[(Tpmen)Fe(MeCN)]^{2+}$ appears within ~20 min (Supporting Information, Figure S3).

The CO-releasing behavior of **1** in MeCN (and DMF) depends critically on the presence of dioxygen in solution. As mentioned above, **1** does not lose CO in degassed MeCN. Indeed, both the ν_{CO} value (1972 cm^{-1}) and the Fe−C(O) distance of **1** (1.775 (3) Å) indicate a stronger Fe-CO bond compared to that in the other two carbonyls. However, in aerated MeCN, **1** readily loses CO (within ~15 min) much like **2** and **3**. Interestingly, the absorption spectrum (λ_{max} at 470 and 390 nm) of **1** changes to that of the oxo-bridged diiron(III) species $[(PaPy_3)FeOFe(PaPy_3)](ClO_4)_2$ (λ_{max} at 430 and 330 nm, shoulder at 520 nm)[27d] upon such CO release (eq 1a). It is thus evident that formation of the highly stable oxo-bridged diiron species allows the release of CO from **1** in aerated MeCN solution. The stronger tendency of $PaPy_3H$, a ligand with a carboxamide group, toward stabilization of the +3 oxidation state of iron[27,42] drives the reaction in a completely different pathway in presence of dioxygen and makes **1** an efficient CORM in aerated MeCN (and DMF). Since the other two ligands namely $SBPy_3$ and Tpmen, are more supportive of the +2 oxidation state of iron, CO release from **2** and **3** gives rise to the solvated Fe(II) product in solution (eq 1b) both under anaerobic and aerobic conditions.

$$[(PaPy_3)Fe(CO)]^{2+} \xrightarrow[\text{Degassed MeCN}]{} \text{No CO loss} \qquad (1)$$

$$[(PaPy_3)Fe(CO)]^{2+} \xrightarrow[\text{MeCN, air}]{} [(PaPy_3)FeOFe(PaPy_3)]^{2+} \qquad (1a)$$

$$[(L)Fe(CO)]^{n+} \xrightarrow[\text{Solvent (Solv) MeCN, DMF, } H_2O]{L = SBPy_3, \text{ Tpmen}} [(L)Fe(Solv)]^{n+} + CO \qquad (1b)$$

The CO-releasing properties of **1**−**3** have also been studied in aqueous phosphate buffer (PBS, pH 7.4) to assess their utility in biological experiments. As shown in Figure 4, smooth release of CO from **2** causes a red shift of the 450 nm band to 572 nm with the emergence of a new band with λ_{max} at 400 nm. Clean isosbestic points are also observed at 496 and 430 nm. With **3**, a similar red shift of the 330 nm band to 400 nm is noted upon CO release in solution (isosbestic point at 370 nm). The similarities between the final spectra of **2** and **3** in PBS and MeCN suggest that the end products are most possibly the aqua species $[(L)Fe(H_2O)]^{2+}$ (L = $SBPy_3$, Tpmen) in these reactions.

Kinetic Measurements. The utility of the metal carbonyls as CORMs depends critically on the apparent rates of CO loss (k_{CO}) under physiological conditions. In the present work we have determined the k_{CO} values of **1**−**3** in PBS (pH 7.4). The CO release from the carbonyls was followed by recording the electronic spectra of the samples within 1 min of dissolution in phosphate buffer and the absorbance values at specific absorption maximum (405 nm for **1**, 450 nm for **2**, and 330 nm for **3**) were noted versus time (in seconds). For all three carbonyls, CO release obeys a pseudofirst order behavior in aqueous buffer (and MeCN, Supporting Information, Figure S4). The kinetic plot of the apparent rate of CO loss by **2** is shown in Figure 5. Further decomposition of the solvated species in aqueous media, as noted in the overall decrease of the absorption, occurs only after 45−60 min for these CORMs.

To date, a handful of water-soluble CORMs have been reported that act as fast CO donors. We have compared the k_{CO} value of $[Ru(glycine)(CO)_3Cl]$ (CORM-3),[20] with those of **1**−**3** under similar conditions. The k_{CO} values for **1**−**3** are 1.3×10^{-3} s^{-1}, 7.5×10^{-4} s^{-1}, and 3.7×10^{-3} s^{-1}, respectively. Under comparable conditions, CORM-3 affords a k_{CO} value of 1.5×10^{-3} s^{-1}. It thus appears that **2** releases CO more slowly over a longer period of time compared to CORM-3 while the k_{CO} values of **1** and CORM-3 are quite comparable. The k_{CO} values of **2** and **3** in MeCN (1.3×10^{-3} s^{-1} and 6.3×10^{-3} s^{-1} respectively) are consistently faster than the values in aqueous buffer. This difference could arise from the fact that MeCN is a better donor for the Fe(II) center ligated to polypyridine ligand.[36]

Delivery of CO to Myoglobin. The designed carbonyls readily deliver CO to reduced myoglobin (Mb) under physiological conditions. Because the carbonyls start release of CO

dx.doi.org/10.1021/ic2000848 |*Inorg. Chem.* 2011, 50, 3127–3134

immediately upon dissolution, an excess (7−8 fold based on the amount of Mb) of each compound in PBS (pH 7.4) was required to completely convert reduced Mb to carbonyl myoglobin (Mb-CO) with solutions of the CORMs in such reactions. The rapid formation of Mb-CO was apparent within 1 min of addition as evidenced by the shift of the Soret band from 435 to 424 nm (Figure 6). Mb-CO production levels off after 20 min in the case of **2** and 24 min for **3**, with the final absorbance readings taken at 30 min. While kinetic measurements predict a slower rate of CO release for **2** compared to **3**, the Mb-based CO release test shows that both carbonyls generate CO at a similar rate over the same period of time. These resulting half-lives, defined as the time during which Mb-CO formation is 50% complete (∼ 8 min for both species), are comparable to known CORMs that release CO when dissolved. For instance, CORM-3 was reported to have a half-life of 4−18 min,[20] while some Cr-based CORMs employing amino acids and amino ester ligands have half-lives of 7−9 min.[24]

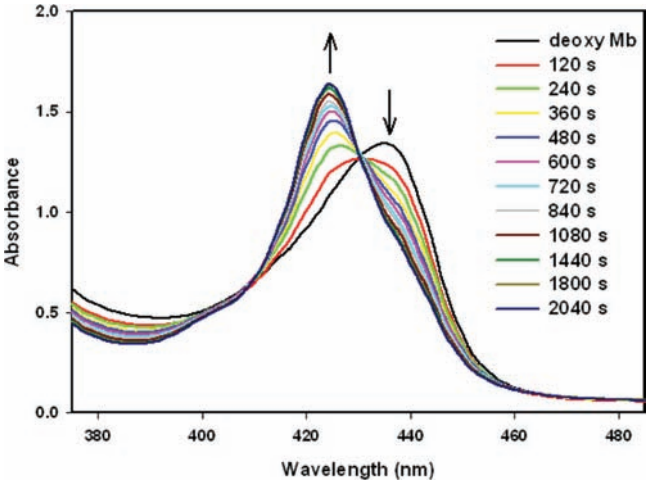

Figure 6. Delivery of CO from **3** to reduced Mb (λ_{max} = 435 nm), resulting in Mb-CO adduct (λ_{max} = 424 nm) in PBS pH 7.4.

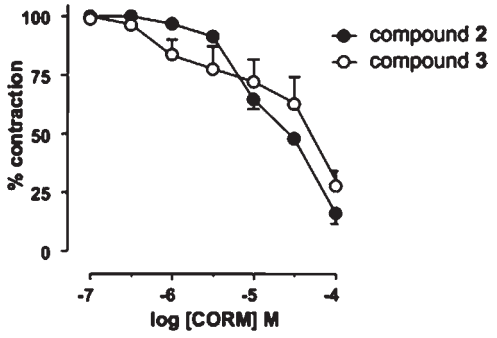

Figure 7. Vasorelaxation of mouse aorta muscle ring using **2** and **3** as a function of concentration.

Vasorelaxation of Mouse Aorta. The vasorelaxation property of CO has been a subject of debate in relation to its binding and activating to sGC and the concomitant cGMP pathway. Despite low affinity of CO to sGC,[12] relaxation of smooth muscle by CO via cGMP pathway has been proposed.[18,21] In the present study, we have examined the effect(s) of CO release from the present carbonyls on mouse aorta muscle rings in tissue bath experiments. Both **2** (30 nM−100 μM) and **3** (30 nM−300 μM) produced concentration-dependent relaxations with EC_{50} values of 3.4 ± 0.2 μM and 26.2 ± 0.2 μM, respectively (Figure 7). These values are superior to values obtained with CORM-3 reported by Motterlini and co-workers.[21] Interestingly, we did not observe much inhibitory effect by ODQ, a common sGC inhibitor (Figure 8). In previous work, Motterlini and co-workers have reported initial inhibition by ODQ which was eventually lost after repeated addition of CORM-3.[21]

It has been postulated that smooth muscle relaxation by CO could arise from its binding to the channel-bound heme of the large-conductance Ca^{2+}-activated K-channel (BK_{Ca}).[14b,43,44] To test this hypothesis, we studied the effect of the BK_{Ca} channel blocker iberiotoxin on the inhibition of vasorelaxation by **3**. Significant inhibition was indeed observed with this BK_{Ca} channel blocker while no effect was noted with the K_{ATP} channel blocker glibenclamide or the nonselective K^+-channel blocker TEA (data not shown). Clearly, more studies are required to determine the origin of vasorelaxation of smooth muscle by these CORMs. Nevertheless, the excellent vasorelaxation effects of **2** and **3** merit attention as new CORMs that could be used to deliver CO under physiological conditions. Further studies on the mechanism of vasorelaxation by these CORMs are in progress in this laboratory.

SUMMARY AND CONCLUSIONS

The following are the summary and conclusions of this work.

(a) Three structurally related Fe(II) carbonyls **1**−**3** have been synthesized from designed polypyridine ligands and characterized by spectroscopy and X-ray crystallography. The structure of **1** has been reported by us in a previous account.[36]

(b) In aqueous and nonaqueous solutions, these carbonyls rapidly release CO and hence can act as potential CORMs.

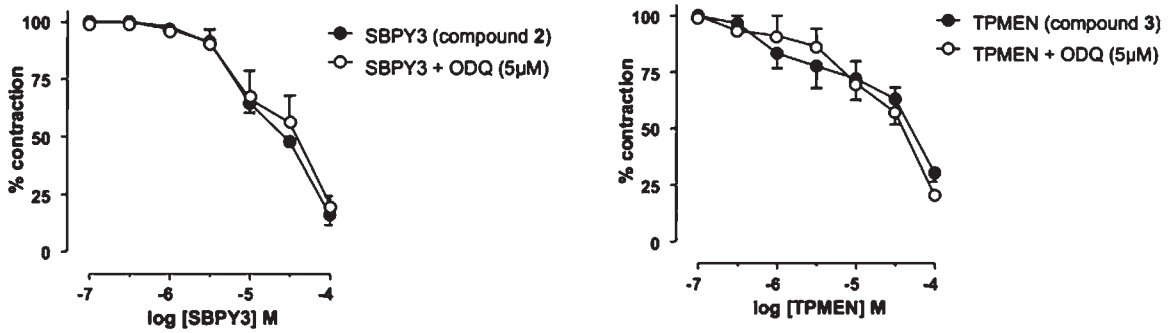

Figure 8. Vasorelaxation of mouse aorta muscle rings by **2** and **3** in the absence and presence of ODQ (5 μM).

dx.doi.org/10.1021/ic2000848 |*Inorg. Chem.* 2011, 50, 3127–3134

(c) Both **2** and **3** have been employed to deliver CO to myoglobin under physiological conditions.

(d) **2** and **3** exhibit excellent vasorelaxation in mouse aorta muscle rings in tissue-bath experiments. The relaxation effect is not inhibited by ODQ, an sGC inhibitor. However, significant inhibition is observed with the BK_{Ca} channel blocker iberiotoxin.

■ ASSOCIATED CONTENT

Supporting Information. X-ray crystallographic data (in CIF format) for $[(SBPy_3)Fe(CO)](BF_4)_2$ (**2**) and preliminary structure of $[(Tpmen)Fe(CO)](ClO_4)_2$ (**3**, Figure S1), changes in the electronic absorption spectra of **2** and **3** in MeCN (Figures S2 and S3), plot of changes in ln(Absorbance) of **2** versus time in MeCN (Figure S4). This material is available free of charge via the Internet at http://pubs.acs.org.

■ AUTHOR INFORMATION

Corresponding Author

*E-mail: pradip@chemistry.ucsc.edu.

■ ACKNOWLEDGMENT

This research was supported by the NSF Grant CHE-0957251. M.G. was supported by the IMSD Grant GM-58903 and the NHGRI Grant HG002371. We thank Drs. Marilyn Olmstead and Allen Oliver for help in crystallographic studies. The ALS is supported by the U.S. Department of Energy, Office of Energy Sciences Materials Sciences Division, under contract DE-AC02-05CH11231.

■ REFERENCES

(1) *Signal Transduction and the Gasotransmitters: NO, CO and H2S in Biology and Medicine*; Wang, R., Ed.; Humana Press: Totowa, NJ, 2004.

(2) Ignarro, L. J. *Nitric Oxide: Biology and Pathobiology*; Academic Press: San Diego, 2000.

(3) *Nitric Oxide Free Radicals in Peripheral Neurotransmission*; Kalsner, S., Ed.; Birkhauser: Boston, 2000.

(4) *Nitric Oxide and Infection*; Fang, F. C., Ed.; Kluwer Academic: New York, 1999.

(5) *Nitric Oxide and Cell: Proliferation, Differentiation and Death*; Moncada, S., Higgs, E. A., Bagetta, G., Eds.; Portland Press: London, 1998.

(6) Fukuto, J. M.; Collins, M. D. *Curr. Pharm. Des.* **2007**, *13*, 2952–2978.

(7) Li, L.; Hsu, A.; Moore, P. K. *Pharmacol. Ther.* **2009**, *123*, 386–400.

(8) *The Smallest Biomolecules: Diatomics and their Interactions with Heme Proteins*; Ghosh, A., Ed.; Elsevier: Amsterdam, 2008.

(9) (a) Kaczorowski, D. J.; Zuckerbraun, B. S. *Curr. Med. Chem.* **2007**, *14*, 2720–2725. (b) Kim, H. P.; Ryter, S. W.; Choi, A. M. K. *Annu. Rev. Pharmacol. Toxicol.* **2006**, *46*, 411–449.

(10) Hartsfeield, C. L. *Antioxid. Redox Signaling* **2002**, *4*, 301–307.

(11) Kikuchi, G.; Yoshida, T.; Noguchi, M. *Biochem. Biophys. Res. Commun.* **2005**, *338*, 558–567.

(12) (a) Ma, X.; Sayed, N.; Beuve, A.; van den Akker, F. *EMBO J.* **2007**, *26*, 578–588. (b) Stone, J. R.; Marletta, M. A. *Biochemistry* **1994**, *33*, 5636–5640.

(13) (a) Wang, R. *Can. J. Physiol. Pharmacol.* **1998**, *76*, 1–15. (b) Coceani, F.; Kelsey, L.; Seidlitz, E. *Br. J. Pharmacol.* **1996**, *118*, 1689–1696.

(14) (a) Dong, D.-L.; Zhang, Y.; Lin, D. -H.; Chen, J.; Patschan, S.; Goligorsky, M. S.; Nasjletti, A.; Yang, B. -F.; Wang, W. -H. *Hypertension* **2007**, *50*, 643–651. (b) Jaggar, J. H.; Li, A.; Parfenova, H.; Liu, J.; Umstot, E. S.; Dopico, A. M.; Leffler, C. W. *Circ. Res.* **2005**, *97* (8), 805–812. (c) Wang, R.; Wu, L. *J. Biol. Chem.* **1997**, *272*, 8222–8226.

(15) Otterbein, L. E.; Mantell, L. L.; Choi, A. M. K. *Am. J. Physiol.* **1999**, *276*, L688–L694.

(16) Otterbein, L. E.; Zuckerbraun, B. S.; Haga, M.; Liu, F.; Song, R.; Usheva, A.; Stachular, C.; Bodyak, N.; Smith, R. N.; Csizmadia, E.; Tyagi, S.; Akamatsu, Y.; Flavell, R. J.; Billiar, T. R.; Tzeng, E.; Bach, F. H.; Choi, A. M. K.; Soares, M. P. *Nat. Med.* **2003**, *9*, 183–190.

(17) Suliman, H. B.; Carraway, M. S.; Tatro, L. G.; Piantadosi, C. A. *J. Cell Sci.* **2007**, *120*, 299–308.

(18) (a) Johnson, T. R.; Mann, B. E.; Clark, J. E.; Foresti, R.; Green, C. J.; Motterlini, R. *Angew. Chem., Int. Ed.* **2003**, *42*, 3722–3729. (b) Motterlini, R.; Clark, J. E.; Foresti, R.; Sarathchandra, P.; Mann, B. E.; Green, C. J. *Circ. Res.* **2002**, *90*, e17–e24.

(19) Zhang, W. Q.; Atkin, A. J.; Thatcher, R. J.; Whitwood, A. C.; Fairlamb, I. J. S.; Lynam, J. M. *Dalton Trans.* **2009**, 4351–4358.

(20) Clark, J. E.; Naughton, P.; Shurey, S.; Green, C. J.; Johnson, T. R.; Mann, B. E.; Foresti, R.; Motterlini, R. *Circ. Res.* **2003**, *93*, e2–e8.

(21) Foresti, R.; Hammad, J.; Clark, J. E.; Johnson, T. R.; Mann, B. R.; Friebe, A.; Green, C. J.; Motterlini, R. *Br. J. Pharmacol.* **2004**, *142*, 453–460.

(22) Alberto, R.; Motterlini, R. *Dalton Trans.* **2007**, 1651–1660.

(23) Zhang, W. Q.; Whitwood, A. C.; Fairlamb, I. J. S.; Lynam, J. M. *Inorg. Chem.* **2010**, *49*, 8941–8952.

(24) Sawle, P.; Hammad, J.; Fairlamb, I. J. S.; Moulton, B.; O'Brien, C. T.; Lynam, J. M.; Duhme-Klair, A. K.; Foresti, R.; Motterlini, R. *J. Pharmacol. Exp. Ther.* **2006**, *318*, 403–410.

(25) Niesel, J.; Pinto, A.; N'Dongo, H. W. P.; Merz, K.; Ott, I.; Gust, R.; Schatzschneider, U. *Chem. Commun.* **2008**, 1798.

(26) Metal carbonyls such as $[Mn_2(CO)_{10}]$[21] and $[Fe(CO)_5]$[22] are known to give off CO through photodissociation. See Zhang, S.; Zhang, H. T.; Brown, T. L. *Organometallics* **1992**, *11*, 3929. Waller, I. M.; Davis, H. F.; Hepburn, J. W. *J. Phys. Chem.* **1987**, *91*, 506.

(27) (a) Eroy-Reveles, A. A.; Hoffman-Luca, C. G.; Mascharak, P. K. *Dalton Trans.* **2007**, 5268–5274. (b) Patra, A. K.; Rose, M. J.; Olmstead, M. M.; Mascharak, P. K. *J. Am. Chem. Soc.* **2004**, *126*, 4780–4781. (c) Patra, A. K.; Rowland, J. M.; Marlin, D. S.; Bill, E.; Olmstead, M. M.; Mascharak, P. K. *Inorg. Chem.* **2003**, *42*, 6812–6823. (d) Patra, A. K.; Afshar, R.; Olmstead, M. M.; Mascharak, P. K. *Angew. Chem., Int. Ed.* **2002**, *41*, 2512–2515.

(28) (a) Hoffman-Luca, C. G.; Eroy-Reveles, A. A.; Alvarenga, J.; Mascharak, P. K. *Inorg. Chem.* **2009**, *48*, 9104–9111. (b) Ghosh, K.; Eroy-Reveles, A. A.; Holman, T. R.; Olmstead, M. M.; Mascharak, P. K. *Inorg. Chem.* **2004**, *43*, 2988–2997.

(29) (a) Rose, M. J.; Mascharak, P. K. *Coord. Chem. Rev.* **2008**, *252*, 2093–2114. (b) Rose, M. J.; Mascharak, P. K. *Curr. Opin. Chem. Biol.* **2008**, *12*, 238–244.

(30) (a) Rose, M. J.; Patra, A. K.; Olmstead, M. M.; Mascharak, P. K. *Inorg. Chem.* **2007**, *46*, 2328–2338. (b) Patra, A. K.; Rose, M. J.; Murphy, K. A.; Olmstead, M. M.; Mascharak, P. K. *Inorg. Chem.* **2004**, *43*, 4487–4495. (c) Patra, A. K.; Mascharak, P. K. *Inorg. Chem.* **2003**, *42*, 7363–7365.

(31) (a) Rose, M. J.; Mascharak, P. K. *Inorg. Chem.* **2009**, *48*, 6904–6917. (b) Rose, M. J.; Olmstead, M. M.; Mascharak, P. K. *J. Am. Chem. Soc.* **2007**, *129*, 5342–5343.

(32) (a) Eroy-Reveles, A. A.; Mascharak, P. K. *Future Med. Chem.* **2009**, *1* (8), 1497–1507. (b) Eroy-Reveles, A. A.; Leung, Y.; Beavers, C. M.; Olmstead, M. M.; Mascharak, P. K. *J. Am. Chem. Soc.* **2008**, *130*, 4447–4458. (c) Eroy-Reveles, A. A.; Leung, Y.; Mascharak, P. K. *J. Am. Chem. Soc.* **2006**, *128*, 7166–7167.

(33) (a) Madhani, M.; Patra, A. K.; Miller, T. W.; Eroy-Reveles, A. A.; Hobbs, A.; Fukuto, J. M.; Mascharak, P. K. *J. Med. Chem.* **2006**, *49*, 7325–7330. (b) Szundi, I.; Rose, M. J.; Sen, I.; Eroy-Reveles, A. A.; Mascharak, P. K.; Einarsdottir, O. *Photochem. Photobiol.* **2006**, *82*, 1377–1384. (c) Afshar, R. K.; Patra, A. K.; Mascharak, P. K. *J. Inorg. Biochem* **2005**, *99*, 1458–1464.

(34) Rose, M. J.; Fry, N. L.; Marlow, R.; Hinck, L.; Mascharak, P. K. *J. Am. Chem. Soc.* **2008**, *130*, 8834–8846.
(35) (a) Halpenny, G. M.; Gandhi, K. R.; Mascharak, P. K. *ACS Med. Chem. Lett.* **2010**, *1*, 180–183. (b) Halpenny, G. M.; Steinhardt, R. C.; Okialda, K. A.; Mascharak, P. K. *J. Mater. Sci: Mater. Med.* **2009**, *20*, 2353–2360.
(36) Afshar, R. K.; Patra, A. K.; Bill, E.; Olmstead, M. M.; Mascharak, P. K. *Inorg. Chem.* **2006**, *45*, 3774–3781.
(37) Patra, A. K.; Olmstead, M. M.; Mascharak, P. K. *Inorg. Chem.* **2002**, *41*, 5403–5409.
(38) Bernal, I.; Jensen, I. M.; Jensen, K. B.; McKenzie, C. J.; Toftlund, H.; Tuchagues, J.-P. *J. Chem. Soc., Dalton Trans.* **1995**, 3667–3675.
(39) Sugimoto, H.; Sawyer, D. T. *J. Am. Chem. Soc.* **1985**, *107*, 5712–5716.
(40) Salzmann, R.; Ziegler, C. J.; Godbout, N.; McMahon, M. T.; Suslick, K. S.; Oldfield, E. *J. Am. Chem. Soc.* **1998**, *120*, 11323–11334.
(41) Vaska, L.; Yamaji, T. *J. Am. Chem. Soc.* **1971**, *93*, 6673–6674.
(42) Marlin, D. S.; Mascharak, P. K. *Chem. Soc. Rev.* **2000**, *29*, 69–74.
(43) Horrigan, F. T.; Heinemann, S. H.; Hoshi, T. *J. Gen. Physiol.* **2005**, *126*, 7–21.
(44) Wang, R.; Wu, L.; Wang, Z. *Pflugers Arch.- Eur. J. Physiol.* **1997**, *434*, 285–291.